Catalysis Today 148 (2009) 323–328

Contents lists available at ScienceDirect

Catalysis Today

journal homepage: www.elsevier.com/locate/cattod

Crystal structures, acid–base properties, and reactivities of $Ce_xZr_{1-x}O_2$ catalysts

Wei Wang [a], Shengping Wang [a], Xinbin Ma [a,*], Jinlong Gong [b,**]

[a] Key Laboratory for Green Chemical Technology, School of Chemical Engineering and Technology, Tianjin University, Weijin Road 92, Nankai District, Tianjin 300072, China
[b] Department of Chemistry and Chemical Biology, Harvard University, Cambridge, MA 02138, USA

ARTICLE INFO

Article history:
Available online 19 August 2009

Keywords:
Diethyl carbonate
CO_2
Ethanol
Direct synthesis
$Ce_xZr_{1-x}O_2$
Acid–base sites

ABSTRACT

Direct synthesis of diethyl carbonate from ethanol and CO_2 is attractive since starting materials are cheap and easily obtainable, and the initial operational procedures are quite simple. We present results showing that $Ce_xZr_{1-x}O_2$ solid solution catalysts are effective and selective for producing diethyl carbonate and could be recyclable without loss of any activity. High calcination temperature is favorable based on results of catalytic test. X-ray diffraction and temperature-programmed desorption of NH_3 and CO_2 provide evidence indicating that catalytic properties of $Ce_xZr_{1-x}O_2$ are closely dependent on the crystal structures and the acid–base sites on the surface with varied Ce/Zr ratios. Strong acid–base sites on the surfaces of catalysts are unfavorable for diethyl carbonate formation.

© 2009 Elsevier B.V. All rights reserved.

1. Introduction

Diethyl carbonate (DEC), one of the most important carbonates, has been widely used as environmentally benign intermediate and raw material in chemical industry [1]. In addition, DEC has been considered as a better candidate than dimethyl carbonate (DMC) and ethanol for replacing methyl ter-butyl ether (MTBE) as the additive to gasoline [2]. Therefore, synthesis of DEC attracts much attention. Traditionally, DEC is synthesized via phosgene as a raw material [3]; however, phosgene is a toxic species, which causes an undesired environmental impact due to the high energy demand for the synthesis of chlorine as well as the disposal of large amount of chlorinated solvents and inorganic chloride.

In order to achieve the principles of "Green Chemistry" that aim at the lowest impacts on human health and environment, many other alternatives have been proposed and investigated. One of these methods is a process based on oxidative carbonylation of ethanol with carbon monoxide and oxygen catalyzed by cuprous chloride (Eqs. (1) and (2)) [4,5].

$$2CH_3CH_2OH + 1/2O_2 + CuCl \rightarrow Cu(OCH_2CH_3)Cl + H_2O \quad (1)$$

$$Cu(OCH_2CH_3)_2Cl + CO \rightarrow (CH_3CH_2O)_2CO + 2CuCl \quad (2)$$

The UBE Industry developed another phosgene-free process for DEC synthesis using a palladium catalyst and an ethyl nitrite promoter [6]. The reaction is represented as follows.

$$2CH_3CH_2OH + 2NO + (1/2)O_2 \rightarrow 2CH_3CH_2ONO + H_2O \quad (3)$$

$$2CH_3CH_2ONO + CO \rightarrow (CH_3CH_2O)_2CO + 2NO \quad (4)$$

More importantly, chemical fixation and application of carbon dioxide (CO_2) has recently received much attention primarily due to its potential use as an abundant carbon source and its indirect role as an environmental pollutant [7,8]. This approach can contribute to the development of new clean synthetic methodologies, avoiding using of toxic substances and producing of waste as well as implementing the principle of atom-economy and energy saving. Accordingly, a direct procedure of synthesis of diethyl carbonate from CO_2 and ethanol (Eq. (5)) has been developed.

$$2CH_3CH_2OH + CO_2 \rightarrow (CH_3CH_2O)_2CO + H_2O \quad (5)$$

For a similar reaction, ceria–zirconia ($Ce_xZr_{1-x}O_2$) solid solution as a catalyst has been studied for selective synthesis of dimethyl carbonate (DMC) from methanol and CO_2 [9,10]. It has been shown that $Ce_xZr_{1-x}O_2$ has both acid and base sites [11,12], which play an important role in catalytic performance [13,14]. Moreover, depending on the Ce/Zr ratios and calcination temperatures, different crystal structures of $Ce_xZr_{1-x}O_2$ were observed [15–21]. Tomishige et al. showed a dependence of DEC yield from C_2H_5OH and CO_2 over $Ce_{0.2}Zr_{0.8}O_2$ and CeO_2 on reaction time and catalyst weight [10,22]. When 0.1 g, 0.5 g, 1.4 g $Ce_{0.2}Zr_{0.8}O_2$, or 0.1 g CeO_2 catalyst was used, DEC yield was almost same (0.4 mmol) after an appropriate reaction time, and the amount of by-products was below the detection limit of FID-GC. These results indicate that the equilibrium level of DEC formation from C_2H_5OH and CO_2 is achieved in this reaction system. However, few studies have been

* Corresponding author. Tel.: +86 22 2740 6498; fax: +86 22 8740 1818.
** Corresponding author. Tel.: +1 617 495 9435.
E-mail addresses: xbma@tju.edu.cn (X.B. Ma), gong@fas.harvard.edu (J.L. Gong).

0920-5861/$ – see front matter © 2009 Elsevier B.V. All rights reserved.
doi:10.1016/j.cattod.2009.07.090

reported regarding the crystal structures and acid–base properties of $Ce_xZr_{1-x}O_2$ for the direct synthesis of DEC from ethanol and carbon dioxide. Therefore, a systematic approach to better understanding this issue would be greatly useful.

In this paper, we present results from an investigation of crystal structures, physicochemical properties, and reactivities of $Ce_xZr_{1-x}O_2$ catalysts prepared by a co-precipitation method with tunable Ce/Zr ratios under various calcination temperatures. A relation between activities and catalyst properties was examined employing BET, X-ray diffraction (XRD), X-ray photoelectron spectroscopy (XPS), and temperature-programmed desorption of ammonia and carbon dioxide (NH_3-TPD and CO_2-TPD).

2. Experimental

2.1. Catalyst preparation

$Ce_xZr_{1-x}O_2$ catalysts were prepared at room temperature by a co-precipitation method with aqueous solutions of $ZrOCl_2{\cdot}8H_2O$ and $Ce(NO_3)_3{\cdot}6H_2O$ in desired quantities using aqueous ammonium hydroxide as a precipitator. pH value during this procedure was controlled to be about 10. The resultant precipitate was collected and washed with deionized water until Cl species was undetectable by an $AgNO_3$ solution. The as-prepared sample was dried overnight at 393 K and calcined at different temperature (673–1273 K) for 5 h in air.

2.2. DEC synthesis from ethanol and CO_2

Regarding catalytic test, 257 mmol CH_3CH_2OH and 0.5 g catalyst were added into a 100 mL stainless steel autoclave reactor followed by purging the reactor with CO_2 to a pressure up to 5 MPa (238 mmol CO_2). The reactor was heated and stirred constantly at desired temperature (i.e., 413 K) during the reaction. The total pressure at 413 K was about 8 MPa. After the reaction, the reactor was cooled to room temperature and depressurized. In order to quantitatively analyze composition of the mixture, 1-propanol was added as a standard substance. The products were analyzed by a gas chromatograph (FID-GC, Agilent 4890D) with a capillary column (Agilent HP-5). Under reaction conditions, DEC was the main product with a trace amount of aldehydes and acetal as by-products.

2.3. Catalyst characterization

Surface areas were determined on a constant volume adsorption apparatus (Micromeritics Gemini) by the N_2 BET method at liquid nitrogen temperature. Prior to the measurements, all samples were degassed at 363 K for 3 h.

XRD spectra of catalysts were acquired by an X-ray diffractometer (D/Max-2500) using Cu Kα (40 kV, 100 mA) radiation with a 2θ ranging from 10° to 80° at a scanning speed of 8°/min.

X-ray photoelectron spectroscopy (XPS) spectra were obtained using a spectrometer (Perkin-Elmer PHI 1600), equipped with a microspot monochromatised Al Kα source and a gun of low energy electrons for compensation of electrostatic charging of samples. The Al Kα line (1486.6 eV) was used throughout this work and the base pressure of the chamber was below 1.6×10^{-8} Pa. The values of binding energies BE (eV) were taken relatively to the binding energy of Cls electrons of hydrocarbons on the sample surface (produced by adventitious carbon), which is accepted to be equal to 284.6 eV.

Temperature-programmed desorption (TPD) of ammonia and carbon dioxide was used to determine the acid–base properties of catalysts. TPD experiments were carried out on a flow apparatus (Micromeritics 2910) with a procedure as follows. The catalyst sample (100 mg) was pretreated at 473 K in an argon flow at a rate of 30 mL/min for 40 min and saturated with a pure NH_3 or CO_2 flow after cooling to 323 K. These pretreated samples were purged with argon gas at 323 K for 30 min at a flow rate of 30 mL/min to remove physisorbed NH_3 or CO_2 and then heated to 1223 K at a rate of 10 K/min in a helium flow.

Table 1
Dependence of Ce content in $Ce_xZr_{1-x}O_2$ catalysts on yield and selectivity of DEC and BET surface area.

Entry	Ce content x	DEC yield (mmol)	DEC selectivity (%)	BET surface area (m^2/g)
1	0	0.20	80	51
2	0.07	0.28	90	98
3	0.15	0.21	80	39
4	0.25	0.14	57	39
5	0.5	0.14	57	38
6	0.8	0.17	67	49
7	1	0.40	94	17

Reaction conditions: reaction temperature, 413 K; CH_3CH_2OH:CO_2 = 257:238 mmol; reaction time, 2 h; catalyst weight, 0.5 g; calcination temperature, 1073 K.

3. Results and discussion

3.1. DEC synthesis from ethanol and CO_2

Table 1 shows the relationship between Ce content in $Ce_xZr_{1-x}O_2$ catalysts (calcined at 1073 K) and DEC selectivity and yield and BET surface area. Under operational conditions, CeO_2 (x = 1) exhibited the highest activity regarding DEC yield and selectivity followed by $Ce_{0.07}Zr_{0.93}O_2$ (x = 0.07, entry 2). A possible reason for better performance of CeO_2 and $Ce_{0.07}Zr_{0.93}O_2$, compared ZrO_2 and other Ce/Zr ratios is the differences in the crystal structures and in the acid–base sites as will be discussed later. Notably, BET surface area of CeO_2 is the smallest compared to other catalysts shown in Table 1, primarily due to agglomeration of materials in the catalyst, which can be caused by inhomogeneities in the sintered microstructure at high calcination temperature [23,24]. Additionally, insertion of zirconium atoms into the CeO_2 lattices increases thermal stability of the catalysts that further leads to the formation of high surface area upon annealing at high temperature [25,26]. Notably, the relation between Ce content and DEC yield and BET surface area cannot be unambiguously determined based on the data shown in Table 1.

On the basis of the results of Table 1, we used $Ce_{0.07}Zr_{0.93}O_2$ as the catalyst in the experiments below, which exhibited better

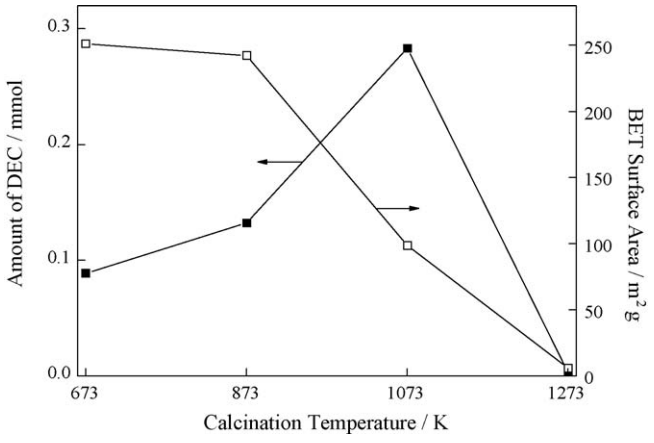

Fig. 1. Dependences of the amount of DEC formation (■) and BET surface area (□) on the calcination temperature over $Ce_{0.07}Zr_{0.93}O_2$ catalysts. Reaction conditions: reaction temperature, 413 K; CH_3CH_2OH:CO_2 = 257:238 mmol; reaction time, 2 h; catalyst weight, 0.5 g.

Table 2
Effects of reaction temperature and time on DEC formation over $Ce_{0.07}Zr_{0.93}O_2$ catalyst.

Entry	Temperature (K)	Time (h)	DEC amount (mmol)	DEC selectivity (%)
1	373	2	0.14	90
2	393	2	0.20	91
3	413	2	0.28	90
4	433	2	0.08	56
5	413	1	0.22	93
6	413	4	0.27	88

Reaction conditions: CH_3CH_2OH:CO_2 = 257:238 mmol; catalyst weight, 0.5 g; calcination temperature, 1073 K.

catalytic performance compared to other Ce/Zr ratios. Fig. 1 shows the dependence of calcination temperature on DEC formed and BET surface area over $Ce_{0.07}Zr_{0.93}O_2$. Indeed, DEC yield increases with increasing calcination temperature and reaches a maximum at 1073 K followed by decreasing to nearly zero at higher calcination temperature (i.e., 1273 K). In addition, BET surface area of the samples decreases with increasing calcination temperature. The similar tendency regarding calcination temperature on CeO_2 catalyst was also observed and for clarification of presentation we will not show the data here.

Effect of reaction temperature (373–433 K) on DEC yield and selectivity over a $Ce_{0.07}Zr_{0.93}O_2$ catalyst has also been investigated and results are shown in Table 2. As can be seen, DEC yield increases with increasing reaction temperature, and reaches a maximum value at 413 K (entry 3). Further increase in temperature to 433 K causes a decrease in DEC production due to the exothermic reaction of DEC formation from ethanol and CO_2 [27]. From thermodynamics point of view, high reaction temperature is not favorable for DEC formation. Additionally, DEC selectivity shows a similar trend as yield, and formation of by-products such as aldehydes and acetal were observed at high reaction temperature. We also briefly investigated dependence of reaction time on reactivity as shown in Table 2. Specifically, 0.22 mmol of DEC are formed in 1 h at 413 K (entry 5), which increases to 0.28 mmol along with the reaction time (i.e., 2 h, entry 3), while DEC selectivity does not change significantly. Interestingly, a further increase of the reaction time to 4 h does not improve DEC yield and selectivity (entry 6), which is probably due to the reaction equilibrium. Additionally, water formed in the reaction could not be removed from the reactor which further affects the reaction process. Molecular sieves (MS) as a dehydrating agent were used to remove the water to shift the equilibrium to DEC. However, all of the attempts have failed presumably due to the high reaction temperature [28].

Based on the results shown in Table 1, CeO_2 and $Ce_{0.07}Zr_{0.93}O_2$ are most reactive, which further motivates us to investigate the effect of the amount of catalyst on the formation of DEC over both catalysts. As shown in Table 3, for 0.1 g, 0.5 g and 1 g $Ce_{0.07}Zr_{0.93}O_2$ catalysts (entries 1, 2 and 3, respectively), amount of formed DEC keeps nearly constant because of reaction equilibrium. However, for a CeO_2 catalyst, DEC yield increases as catalyst amount increases from 0.1 g to 0.5 g (entries 5 and 6). As will discuss below, the activity of 0.1 g CeO_2 catalyst is lower than that of 0.1 g $Ce_{0.07}Zr_{0.93}O_2$ possibly due to the smaller BET surface area. For $Ce_{0.07}Zr_{0.93}O_2$ and CeO_2 catalysts, DEC yield at equilibrium is strongly dependent on the catalysts. This behavior could be ascribed to the difference of dispersion of the active sites on the surfaces of catalysts. The DEC selectivity decreases with increasing catalyst weight when the reaction reached the equilibrium.

Table 3
Effect of catalyst amount on DEC formation over $Ce_xZr_{1-x}O_2$ catalysts[a].

Entry	Ce content x	Catalyst weight (g)	DEC yield (mmol)	DEC selectivity (%)
1	0.07	0.1	0.29	94
2	0.07	0.5	0.28	90
3	0.07	1	0.30	90
4[b]	0.07	0.5	0.30	92
5	1	0.1	0.21	94
6	1	0.5	0.40	94
7	1	1	0.42	92
8[b]	1	0.5	0.42	92

[a] Reaction conditions: reaction temperature, 413 K; CH_3CH_2OH:CO_2 = 257:238 mmol; reaction time, 2 h; calcination temperature, 1073 K.
[b] With used catalyst.

The reusability of $Ce_{0.07}Zr_{0.93}O_2$ and CeO_2 catalysts was also examined. After a reaction run, the catalyst was removed from the reaction system by filtration, washed with acetone, dried at room temperature, and then subjected to the next catalytic run. The results with the used catalysts (entries 4 and 8) are comparable to those obtained with fresh catalysts, indicating that $Ce_{0.07}Zr_{0.93}O_2$ and CeO_2 are recyclable without any loss of activity. The XPS spectra of $Ce_{0.07}Zr_{0.93}O_2$ catalyst before and after the reaction are shown in Fig. 2, where no sensible change was observed on the feature of oxygen, zirconium and cerium. This indicates that the $Ce_{0.07}Zr_{0.93}O_2$ catalyst remains intact after use. We also note that no reduction of Ce(III) takes place [29].

3.2. Characterization of the catalysts

Crystal structures of $Ce_xZr_{1-x}O_2$ catalysts were investigated by XRD and spectra are shown in Fig. 3. Apparently, XRD spectrum of CeO_2 is different from that of ZrO_2. For the catalysts containing both cerium and zirconium, XRD spectra are much closer to that of CeO_2 than ZrO_2, even for high Zr content. Additionally, with the decrease of the Ce content, a shift of the CeO_2 phase peaks toward higher values of 2θ is observed. This phenomenon could be due to the insertion of zirconium atoms in the CeO_2 cubic matrix leading to contraction of parameter of unit cell and deformation of the cubic phase to the tetragonal phase at higher zirconium content [30].

The characteristic peaks at $2\theta = 28.2^\circ$ and 31.5° can be assigned to the monoclinic (M) phase of ZrO_2. The characteristic peak at $2\theta = 30.2^\circ$ represents the tetragonal (T) phase in ZrO_2. For the cubic fluorite (C) phase in CeO_2, XRD peaks at $2\theta = 28.6^\circ$ and 33.1° are evident. It appears that crystal structure is a cubic phase when $x > 0.8$. This structure remains stable with slight modification with $0.15 < x \leq 0.8$. However, for $x \leq 0.15$, cubic phase of $Ce_xZr_{1-x}O_2$ catalysts transforms into a tetragonal phase as well as monoclinic phase. Particularly, intensity of tetragonal phase strengthens with the increase of Zr content. At $x = 0$, both monoclinic phase and tetragonal phase appear.

To further explore thermal properties of $Ce_xZr_{1-x}O_2$ catalysts, we investigated the effect of calcination temperature on crystal structures by XRD. In particular, we select $Ce_{0.07}Zr_{0.93}O_2$ as an example and results are shown in Fig. 4. As can be seen, tetragonal structure is predominant at a calcination temperature of 673 K. Peaks due to both tetragonal and monoclinic structures are observed at temperature above 873 K. At a high calcination temperature, monoclinic peak intensity increases. Therefore, it is very likely that active phase for DEC formation is monoclinic structure based on the comparison between Figs. 1 and 4. Low activity of $Ce_{0.07}Zr_{0.93}O_2$ calcined at 1273 K, which also exhibits monoclinic structure, could be explained from analysis of TPD profiles shown below. We also notice that XRD peaks become sharper for the samples calcined at higher temperature, indicating that the crystal growth proceeds more significantly at higher calcination temperature. This can also explain why BET surface area decreases with increasing calcination temperature as shown in Fig. 1.

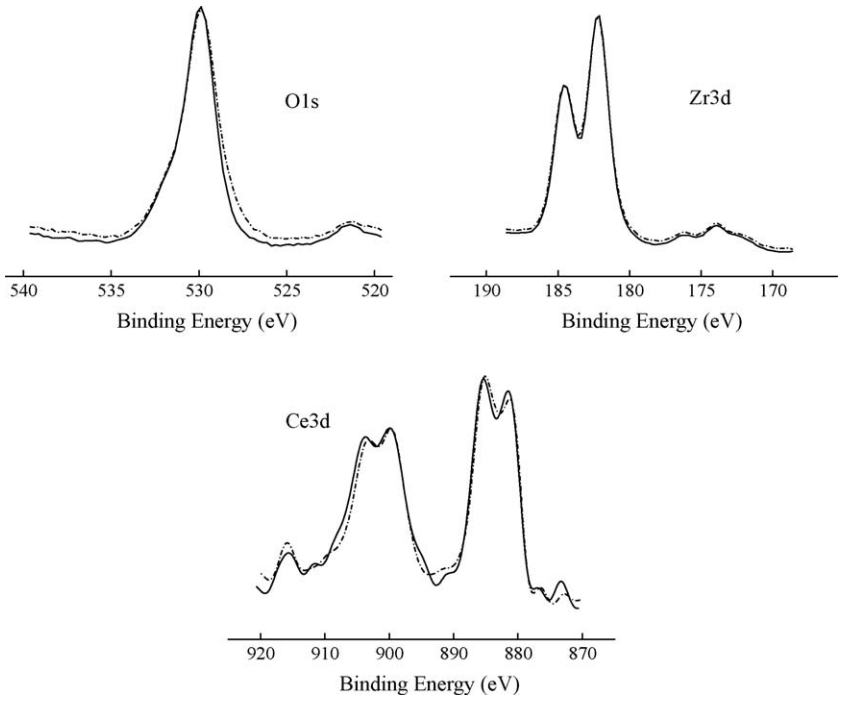

Fig. 2. XPS spectra of $Ce_{0.07}Zr_{0.93}O_2$ catalyst before (continuous line) and after (dotted line) the reaction.

To further explore surface nature of catalysts, particularly acid–base properties, NH_3-TPD and CO_2-TPD were employed and their results are shown in Figs. 5 and 6, respectively. The characteristic peaks of these profiles are assigned to their desorption temperatures indicating the strength of surface sites. In our case, shown in Figs. 5 and 6, both weak and moderate acid–base sites are observed for all catalysts. However, the strong acid–base sites with a characteristic desorption temperature of about 823 K are only observed in the catalysts b–d. $Ce_{0.07}Zr_{0.93}O_2$ and CeO_2 catalysts, which have better reactivity compared to others, do not exhibit any strong acid–base sites. Formation of strong acid–base sites is suggested to be attributed to the presence of metastable tetragonal phase, which leads to the slight modification of cubic crystal structure of the catalyst with $0.15 < x \leq 0.8$. Catalytic performance is depressed by strong acid–base sites on the surface. In the case of direct synthesis of DMC, similar behavior that strong acid–base sites are unsuitable for the production of DMC was also observed on the H_3PO_4/ZrO_2 catalyst [31]. Therefore, activity of $Ce_xZr_{1-x}O_2$ catalysts could be affected by fractions of various crystal structures together with the acid–base sites.

To further investigate the selected $Ce_{0.07}Zr_{0.93}O_2$ catalyst, acid–base properties were examined as a function of calcination temperature employing TPD measurements. Figs. 7 and 8 show TPD profiles of NH_3 and CO_2 adsorbed on $Ce_{0.07}Zr_{0.93}O_2$ calcined at various temperatures, respectively. Note that spectra at 1073 K in Figs. 7 and 8 should be same as those in Figs. 5(a) and 6(a), respectively, but look different due to the different scale. With an increase of the calcination temperature, desorption amount of NH_3

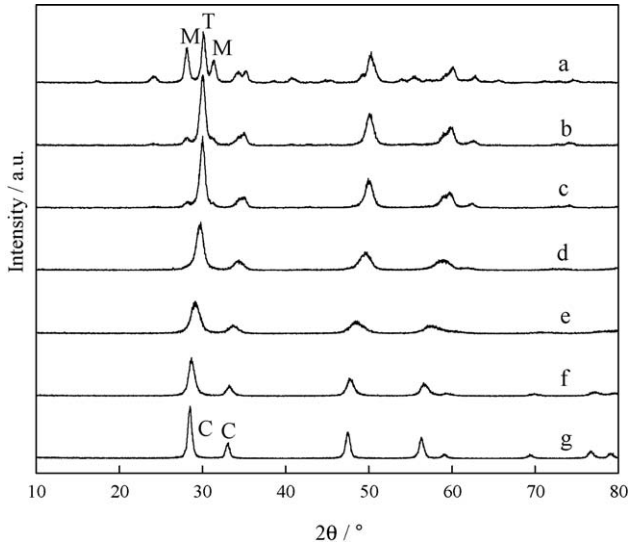

Fig. 3. XRD spectra of $Ce_xZr_{1-x}O_2$ catalysts calcined at 1073 K: (a) $x = 0$, (b) $x = 0.07$, (c) $x = 0.15$, (d) $x = 0.25$, (e) $x = 0.5$, (f) $x = 0.8$ and (g) $x = 1$. Crystal structures: monoclinic (M), tetragonal (T) and cubic fluorite (C).

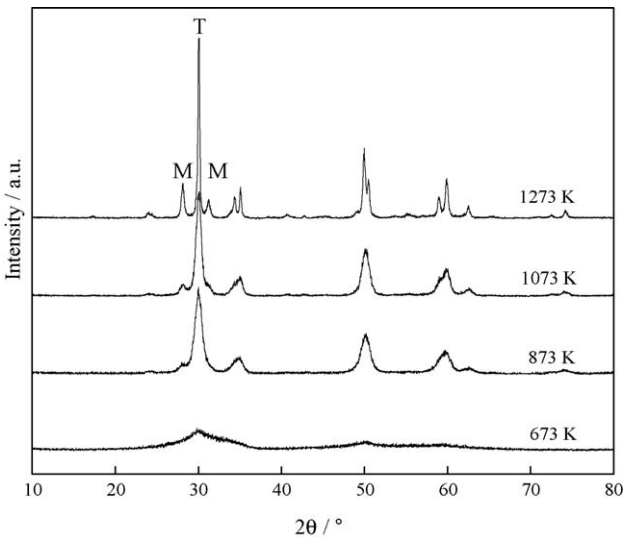

Fig. 4. XRD spectra of $Ce_{0.07}Zr_{0.93}O_2$ catalysts prepared at various calcination temperatures. Crystal structures: monoclinic (M), tetragonal (T) and cubic fluorite (C).

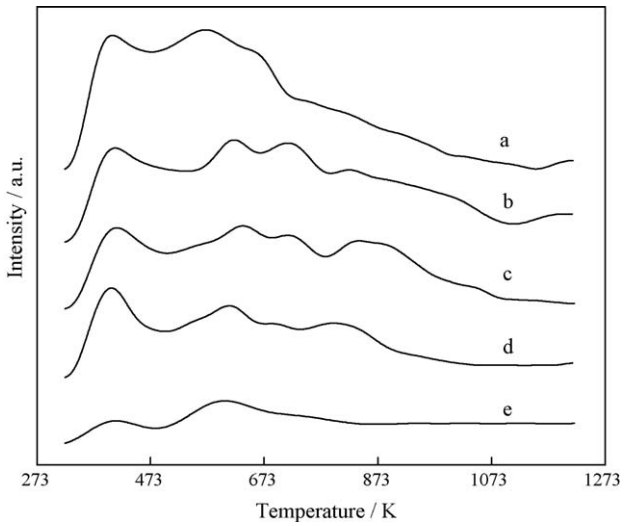

Fig. 5. NH_3-TPD profiles of $Ce_xZr_{1-x}O_2$ catalysts calcined at 1073 K: (a) $x = 0.07$, (b) $x = 0.15$, (c) $x = 0.25$, (d) $x = 0.8$ and (e) $x = 1$.

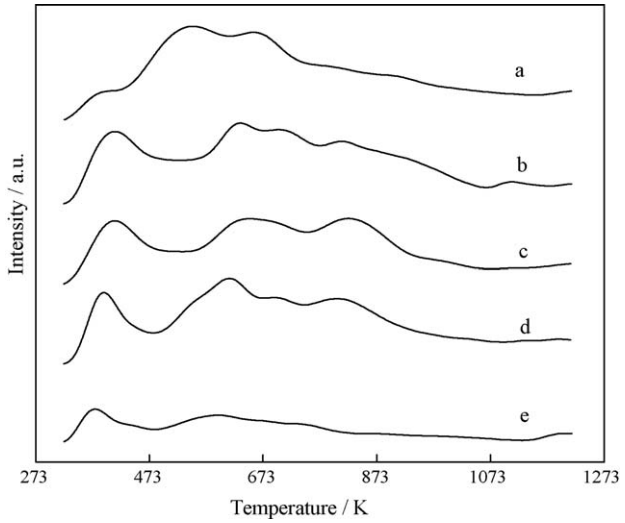

Fig. 6. CO_2-TPD profiles of $Ce_xZr_{1-x}O_2$ catalysts calcined at 1073 K: (a) $x = 0.07$, (b) $x = 0.15$, (c) $x = 0.25$, (d) $x = 0.8$ and (e) $x = 1$.

and CO_2 decreases. Additionally, a shift of desorption peaks toward low temperature can be observed, which is attributed to a decrease of strength of the acidity and basicity with the increase of the calcination temperature. This suggests that the structural change of the surface can make the surface acidity and basicity weaker. Although the details are not clearly elucidated yet, we speculate that the surface of the catalysts calcined at lower temperatures has more roughness and higher temperature calcination makes the surface more plain [32]. There are more coordination unsaturated cations and anions on rougher surfaces, and these sites lead to higher acidity and basicity [33].

From the TPD profiles, we note that a large number of strong basicities and acidities are formed on the surface if calcined at 673 K or 873 K. Moreover, $Ce_{0.07}Zr_{0.93}O_2$ calcined at 1073 K, which shows excellent catalytic activity, does not demonstrate any strong acid–base sites compared to those calcined at 673 K and 873 K. This strongly suggests that strong acid–base sites on the surface are unfavorable for the increase of catalysts activity. On the other hand, catalysts calcined at 1273 K have less acid–base sites suggesting why such catalysts are not active after calcined at high calcination temperature.

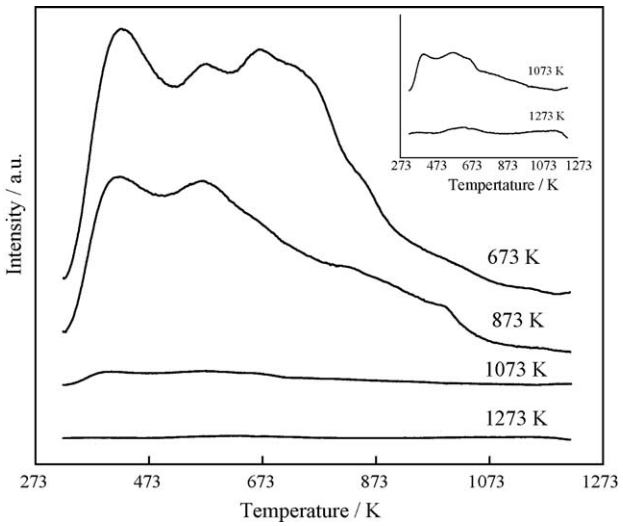

Fig. 7. NH_3-TPD profiles of $Ce_{0.07}Zr_{0.93}O_2$ catalysts prepared at various calcination temperatures.

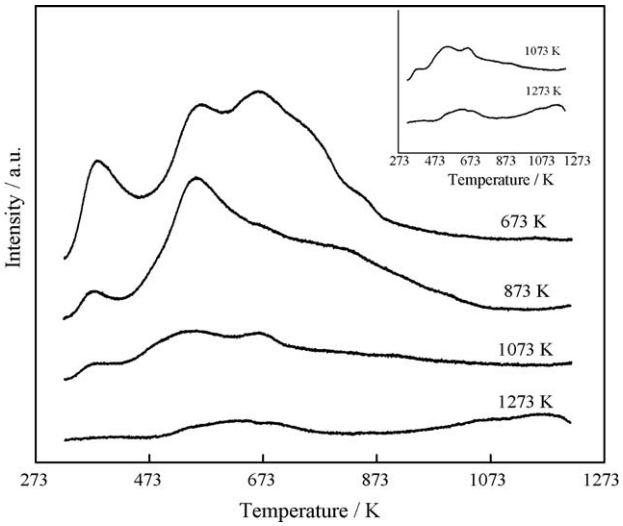

Fig. 8. CO_2-TPD profiles of $Ce_{0.07}Zr_{0.93}O_2$ catalysts prepared at various calcination temperatures.

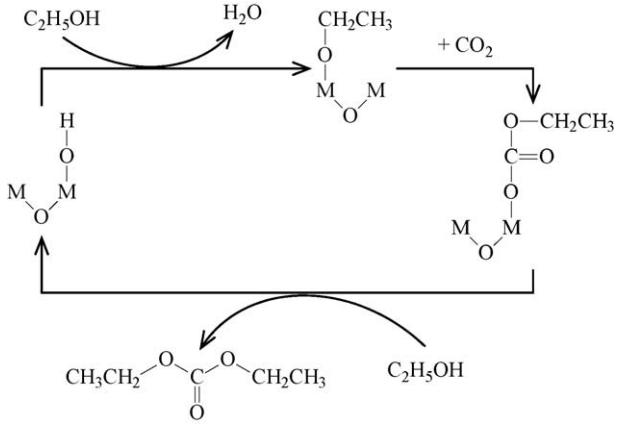

Fig. 9. Proposed mechanism for the direct synthesis of DEC from CO_2 and ethanol over $Ce_xZr_{1-x}O_2$ catalysts.

The mechanism of DMC synthesis from CO_2 and methanol over ZrO_2 catalyst has been proposed according to the results obtained by DRIFT, *in situ* infrared, and *in situ* Raman [13,34,35]. Based on a literature survey and our results, a proposed mechanism of the direct synthesis of DEC from CO_2 and ethanol over $Ce_xZr_{1-x}O_2$ catalysts is shown in Fig. 9, where M stands for the metal site. Ethanol interacts with the unsaturated Lewis acid M^{4+} site (e.g., oxygen vacancy) on the surface of $Ce_xZr_{1-x}O_2$ and releases a proton. This proton could hop along the sites and associate with a surface OH group to form H_2O. CO_2 is then inserted into the M–O bond of the C_2H_5O–M species to produce the reaction intermediate m-C_2H_5OCOO–M. DEC is formed via the further reaction of monoethyl carbonate species with ethanol.

4. Conclusions

We have presented results showing that catalytic properties of $Ce_xZr_{1-x}O_2$ are related to crystal structure and acid–base sites on the surface with varying Ce/Zr ratios. At $0.15 < x \leq 0.8$, the activities of the catalysts decrease due to the formation of strong acid–base sites on the surfaces which are unfavorable for DEC formation. $Ce_{0.07}Zr_{0.93}O_2$ and CeO_2 have higher activity in the direct synthesis of diethyl carbonate from ethanol and CO_2 compared to other Ce–Zr based catalysts. Notably, catalysts could be recyclable without loss of any activity. Particularly, $Ce_{0.07}Zr_{0.93}O_2$ (calcined at 1073 K), consisting of predominant tetragonal phase and a minor monoclinic structure, lacks any strong acid–base sites leading to high reactivity. A plausible reaction mechanism is proposed based on our results and a literature survey.

Acknowledgements

The financial support from the Program for New Century Excellent Talents in University (NCET-04-0242) and the Program of Introducing Talents of Discipline to Universities (No. B06006) are gratefully acknowledged.

References

[1] G. Nagasubramanian, D. Doughty, J. Power Sources 96 (2001) 29.
[2] M.A. Pacheco, C.L. Marshall, Energy Fuels 11 (1997) 2.
[3] I.E. Muskat, F. Strain, U.S. Patent 2,379,250, 1945.
[4] D.M. Fenton, U.S. Patent 3,227,740, 1966.
[5] D.M. Fenton, U.S. Patent 3,227,741, 1966.
[6] S. Umemura, K. Matsui, Y. Ikeda, K. Masunaga, T. Kadota, K. Fujii, K. Nishihira, M. Matsuda, U.S. Patent 4,260,810, 1981.
[7] A. Behr, Angew. Chem. Int. Ed. Engl. 27 (1988) 661.
[8] W. Leitner, Coord. Chem. Rev. 153 (1996) 257.
[9] K. Tomishige, Y. Furusawa, Y. Ikeda, M. Asadullah, K. Fujimoto, Catal. Lett. 76 (2001) 71.
[10] K. Tomishige, K. Kunimori, Appl. Catal. A 237 (2002) 103.
[11] M.G. Cutrufello, I. Ferino, V. Solinas, A. Primavera, A. Trovarelli, A. Auroux, C. Picciau, Phys. Chem. Chem. Phys. 1 (1999) 3369.
[12] K. Watcharapong, J. Bunjerd, A. Suttichai, P. Piyasan, G. Shigeo, Catal. Commun. 8 (2007) 548.
[13] K. Tomishige, Y. Ikeda, T. Sakaihori, K. Fujimoto, J. Catal. 192 (2000) 355.
[14] Y. Ikeda, T. Sakaihori, K. Tomishige, Catal. Lett. 66 (2000) 59.
[15] C. Leitenburg, A. Trovarelli, F. Zamar, S. Maschio, G. Dolcetti, J. Llorca, J. Chem. Soc. Chem. Commun. (1995) 2181.
[16] T. Murota, T. Hasegawa, S. Aozasa, H. Matsui, M. Motoyama, J. Alloys Compd. 193 (1993) 298.
[17] M. Ozawa, M. Kimura, A. Isogai, J. Alloys Compd. 193 (1993) 73.
[18] P. Fornasiero, G. Balducci, M.R. Di, J. Kaspar, V. Sergo, G. Gubitosa, A. Ferrero, M. Graziani, J. Catal. 164 (1996) 173.
[19] Y.T. Moon, H.K. Park, C.H. Kim, J. Am. Ceram. Soc. 78 (1995) 2225.
[20] P. Fornasiero, M.R. Di, R.R. Rango, J. Kaspar, S. Meriani, A. Trovarelli, M. Graziani, J. Catal. 151 (1995) 168.
[21] M. Yashima, H. Arashi, M. Kakihana, M. Yoshimura, J. Am. Ceram. Soc. 77 (1994) 1067.
[22] Y. Yoshida, Y. Arai, S. Kado, K. Kunimori, K. Tomishige, Catal. Today 115 (2006) 95.
[23] D. Terribile, A. Trovarelli, J. Llorca, C. de Leitenburg, G. Dolcetti, Catal. Today 43 (1998) 79.
[24] S.K. Tadokoro, E.N.S. Muccillo, J. Eur. Ceram. Soc. 22 (2002) 1723.
[25] J.R. González-Velasco, M.A. Gutiérrez-Ortiz, J.L. Marc, J.A. Botas, M.P. González-Marcos, G. Blanchard, Appl. Catal. B 25 (2000) 19.
[26] J. Kašpar, P. Fornasiero, J. Solid State Chem. 171 (2003) 19.
[27] L.Q. Zhang, C.F. Zhu, C. Shi, J.F. Wang, Special. Petrochem. 3 (2004) 30.
[28] J.C. Choi, L.N. He, H. Yasuda, T. Sakakura, Green Chem. 4 (2002) 230.
[29] M. Aresta, A. Dibenedetto, C. Pastore, C. Cuocci, B. Aresta, S. Cometa, E.D. Giglio, Catal. Today 137 (2008) 125.
[30] N. Sergent, J. Lamonier, A. Aboukais, Chem. Mater. 12 (2000) 3830.
[31] Y. Ikeda, M. Asadullah, K. Fujimoto, K. Tomishige, J. Phys. Chem. B 105 (2001) 10653.
[32] K. Tomishige, H. Yasuda, Y. Yoshida, M. Nurunnabi, B. Li, K. Kunimori, Green Chem. 6 (2004) 206.
[33] H. Kawakami, S. Yoshida, J. Chem. Soc., Faraday Trans. 2 (80) (1984) 921.
[34] K.T. Jung, A.T. Bell, J. Catal. 204 (2001) 339.
[35] S.B. Xie, A.T. Bell, Catal. Lett. 70 (2000) 137.